751. System identification of rubber-bearing isolators based on experimental tests

Qiang Yin[1, 2], Li Zhou[2], Tengfei Mu[2], Jann N. Yang[3]
[1] School of Mechanical Engineering, Nanjing University of Science and Technology
No. 200 Xiao Ling Wei Street, Nanjing 210094, China
[2] State Key Laboratory of Mechanics and Control of Mechanical Structures
Nanjing University of Aeronautics and Astronautics, China
[3] Department of Civil & Environmental Engineering, University of California, Irvine, CA 92697, USA
E-mail: [1]*yinqiang2009@hotmail.com*

(Received 19 December 2011; accepted 14 February 2012)

Abstract. Rubber-bearing isolation systems have been used in buildings and bridges. These base isolation systems will become more popular in the future due to their ability to reduce significantly the structural responses induced by earthquakes and other dynamic loads. To ensure the integrity and safety of these base isolation systems, a structural health monitoring system is needed. One important problem in the structural health monitoring is the identification of the system and the detection of damages. This problem is more challenging for the rubber-bearing isolation systems because of their nonlinear behavior. In this paper, experimental studies have been conducted for the system identification of nonlinear hysteretic rubber-bearings. Experimental tests of a rubber-bearing isolator under El Centro and Kobe earthquakes have been performed. The Bouc-Wen models with 3, 5 and 6 unknown parameters, respectively, have been investigated to represent the hysteretic behavior of rubber-bearing isolators. The extended Kalman filter (EKF) approach has been used to identify the nonlinear parameters of the Bouc-Wen models for the rubber-bearing isolators. Our experimental studies demonstrate that the Bouc-Wen models are capable of describing the nonlinear behavior of rubber-bearing isolators, and that the EKF approach is effective in identifying nonlinear hysteretic parameters.

Keywords: rubber bearings, hysteretic model, system identification, extended Kalman filter.

Introduction

Base isolation is an innovative performance-based design approach to mitigate earthquake damage potential owing to their excellent performance in reducing the response of structures subject to seismic loads. High damping rubber-bearing isolators have been used in buildings, bridges and other civil structures. In addition, more and more civil infrastructures are expected to be installed with such isolators in the future [1, 2]. The rubber-bearing systems are usually introduced between the superstructure and the foundation to provide lateral flexibility and energy dissipation capacity. A variety of isolation devices, including elastomeric bearings (with and without lead core), have been developed and used for the seismic design of buildings during the last 20 years [3, 4, 5].

To ensure the integrity and safety of these base isolation systems, a structural health monitoring system should be developed. Unfortunately, little has been studied in this important subject area to date. For the health monitoring of rubber-bearing isolators and the corresponding base-isolated structures, one important task is the system identification of these isolators. To accomplish this effort, a suitable nonlinear hysteretic model should be established.

On the other hand, an objective of structural health monitoring systems is to identify the state of the structure and to detect the damage when it occurs. In this regard, analysis techniques for damage identification of structures, based on vibration data measured from sensors, have received considerable attention. A variety of system identification techniques in time domain have been developed for nonlinear and/or multi-degree-of freedom (MDOF) structural systems, such as the least-square estimation (LSE) [6, 7, 8], the extended Kalman filter (EKF) [9, 10, 11], the unscented Kalman filter (UKF) [12], recursive model reference adaptive algorithm [13], and the sequential non-linear least-square estimation (SNLSE) [14, 15], quadratic sum-squares error (QSSE) [16, 17], Monte Carlo filter [18], and wavelet multi-resolution technique [19], etc.

In this experimental study, the Bouc-Wen model is selected to describe the nonlinear behavior of rubber-bearings, which has the advantages of being smooth-varying and physically motivated. Further, experimental tests using a particular type of rubber-bearing (GZN110) have been conducted to identify the parameters of the hysteretic model. Based on experimental data measured from sensors, the EKF method has been used to identify the model parameters. Different earthquake excitations and the Bouc-Wen model with different unknown parameters have been considered. Measured acceleration response data and the EKF approach are used to identify unknown linear and nonlinear parameters. Experimental results demonstrate that the Bouc-Wen model is capable of describing the nonlinear behavior of rubber-bearings, and that the EKF approach is quite effective in identifying the non-linear hysteretic parameters.

Analytical model for rubber-bearing

Several hysteretic models for describing the dynamic behavior of rubber-bearings have been proposed in the literature, including piecewise-linear hysteretic models, polynomial hysteretic models, curvilinear hysteretic models, etc. Among these models, the Bouc-Wen model seems to be more flexible, involving more model parameters to be adjusted. And the hysteresis loop of Bouc-Wen model is smooth and fit the hysteretic character of rubber bearings. So the Bouc-Wen model is adopted to describe the rubber-bearings in this paper.

Consider a single-degree-of freedom hysteretic system (SDOF) excited by a ground acceleration in which x is the relative displacement. The equation of motion can be expressed as:

$$m\ddot{x} + R_T\left(x,z\right) = -m\ddot{x}_0 \tag{1}$$

where z is a hysteretic variable, m is the mass coefficient, and $\ddot{x}_0$ is the ground acceleration. The total restoring force $R_T\left(x,z\right)$ consists of elastic and hysteretic components as follows:

$$R_T\left(x,z\right) = c\dot{x} + \alpha kx + \left(1-\alpha\right)kz \tag{2}$$

where c and k are, respectively, the damping and stiffness coefficients, and $0 \le \alpha \le 1$ is a weighting parameter. The restoring force is purely hysteretic if $\alpha = 0$ and is purely elastic if $\alpha = 1$. A hysteresis model with degradation given by [12, 20] is:

$$\dot{z} = \left(A\dot{x} - \nu\left(\beta\left|\dot{x}\right|\left|z\right|^{n-1}z - \gamma\dot{x}\left|z\right|^{n}\right)\right)/\eta \tag{3}$$

In the above expression, ν and η are degradation shape functions. In general, degradation depends on the response duration and severity. A convenient measure of the combined effect of duration and severity is the hysteretic energy $E\left(t\right) = \int_0^t \left(1-\alpha\right)kz\dot{x}dt$ dissipated through hysteresis from time t = 0 to the present time t. Since the quantity $\varepsilon\left(t\right) = \int_0^t z\dot{x}dt$ is proportional

© VIBROENGINEERING. JOURNAL OF VIBROENGINEERING. MARCH 2012. VOLUME 14, ISSUE 1. ISSN 1392-8716

to $E(t)$, it may also be used as a measure of response duration and severity. Many functional relations between ν, η and ε are possible. From practical considerations, both ν and η are assumed to depend linearly on ε as the system evolves [12, 20]:

$$\nu(\varepsilon) = 1 + \delta_\nu \varepsilon \tag{4}$$

$$\eta(\varepsilon) = 1 + \delta_\eta \varepsilon \tag{5}$$

Two unspecified constant degradation parameters δ_ν and δ_η are thereby introduced.

From Eqs. (1)-(5), there are seven loop parameters (A, α, β, γ, n, δ_ν, δ_η) in the Bouc-Wen model describing the hysteretic behavior. However, it has been shown that A = 1 is quite reasonable, and hence it will be used in this study. Consequently, there remain six parameters (α, β, γ, n, δ_ν, δ_η) in the Bouc-Wen model. To clarify whether every parameter contribute equally to the system response and whether the variations in some parameters combine to annul the effect of each other, attempts were made in the past to understand the influence of each parameter on the system response. For example, Ma, et al. [20] and Yin, et al. [15] studied the sensitivity of the Bouc-Wen model parameters using a one-factor-at-a-time method and provided a graphical representation of the sensitivity ranking. In these loop parameters δ_ν and δ_η are the most insensitive, the rank does not change under different parametric initial values. Thus $\delta_\nu = 0$ and $\delta_\eta = 0$ are adopted in this paper. Then, the unknown hysteresis loop parameters in the Bouc-Wen model are reduced to α, β, γ, n. Chen, et al. [21] used A = 1, $\beta = 0.1$, $\gamma = 0.9$, n = 2 for the laminated and stirruped rubber bearings. Yin, et al. [15] also suggested that A = 1, $\beta = 0.5$, $\gamma = 0.5$, n = 2 for rubber bearings. In this paper, these parameters suggested by Yin, et al. are adopted for a reference and the following experimental results are compared with these suggested values.

Extended Kalman filter

In this section, a brief summary of the extended Kalman filter (EKF) approach is given. Consider a m-DOF structure with the displacement vector, $\boldsymbol{x}$, and velocity vector, $\dot{\boldsymbol{x}}$. Let us introduce an extended state vector, $\boldsymbol{Z}(t) = \{\boldsymbol{x}^{\mathrm{T}}, \dot{\boldsymbol{x}}^{\mathrm{T}}, \boldsymbol{\theta}^{\mathrm{T}}\}^{\mathrm{T}}$, where $\boldsymbol{\theta}^{\mathrm{T}} = [\theta_1, \theta_2, \ldots, \theta_n]^{\mathrm{T}}$ is an n-unknown parametric vector with θ_i (i = 1, 2, …, n) being the ith unknown parameter of the structure, including damping, stiffness, nonlinear and hysteretic parameters. In what follows, the boldface letter represents either a vector or a matrix. The vector equation of motion of the structure can be expressed as:

$$d\boldsymbol{Z}(t)/dt = \boldsymbol{g}(\boldsymbol{Z}, \boldsymbol{f}, t) + \boldsymbol{w}(t) \tag{6}$$

in which $\boldsymbol{w}(t)$ = model noise (uncertainty) vector with zero mean and a covariance matrix $\boldsymbol{Q}(t)$, and $\boldsymbol{f}$ is the excitation vector. A nonlinear discrete vector equation for an observation vector (measured responses) can be expressed as follows:

$$\boldsymbol{Y}_{k+1} = \boldsymbol{h}(\boldsymbol{Z}_{k+1}, \boldsymbol{f}_{k+1}, k+1) + \boldsymbol{v}_{k+1} \tag{7}$$

in which $\boldsymbol{Y}_{k+1}$ is a l-dimensional observation (measured) vector at $t = (k+1)\Delta t$ (sampling time step Δt). In Eq. (7), $\boldsymbol{v}_{k+1}$ is a measurement noise vector assumed to be a Gaussian white noise vector with zero mean and a covariance matrix $E[\boldsymbol{v}_k \boldsymbol{v}_j^{\mathrm{T}}] = \boldsymbol{R}_k \delta_{kj}$, where δ_{kj} is the Kronecker delta.

Let $\hat{\boldsymbol{Z}}_{k+1|k+1}$ be the estimate of $\boldsymbol{Z}_{k+1}$ at $t = (k+1)\Delta t$, and $\hat{\boldsymbol{Z}}_{k+1|k}$ be the estimate of $\boldsymbol{Z}_{k+1}$ at $t = k\Delta t$. The recursive solution for the estimate $\hat{\boldsymbol{Z}}_{k+1|k+1}$ of the extended state vector is given by:

$$\hat{\boldsymbol{Z}}_{k+1|k+1} = \hat{\boldsymbol{Z}}_{k+1|k} + \boldsymbol{K}_{k+1}[\boldsymbol{Y}_{k+1} - \boldsymbol{h}(\hat{\boldsymbol{Z}}_{k+1}, \boldsymbol{f}_{k+1}, k+1)] \tag{8}$$

$$\hat{\boldsymbol{Z}}_{k+1|k} = E\{\hat{\boldsymbol{Z}}_{k+1} \mid \boldsymbol{Y}_1, \boldsymbol{Y}_1, \ldots, \boldsymbol{Y}_k\} = \hat{\boldsymbol{Z}}_{k|k} + \int_{k\Delta t}^{(k+1)\Delta t} \boldsymbol{g}(\hat{\boldsymbol{Z}}_{t|k}, \boldsymbol{f}, t)dt \tag{9}$$

$$\boldsymbol{K}_{k+1} = \boldsymbol{P}_{k+1|k} \boldsymbol{H}_{k+1|k}^{\mathrm{T}} [\boldsymbol{H}_{k+1|k} \boldsymbol{P}_{k+1|k} \boldsymbol{H}_{k+1|k}^{\mathrm{T}} + \boldsymbol{R}_{k+1}]^{-1} \tag{10}$$

In Eq. (10), $\boldsymbol{K}_{k+1}$ is the Kalman gain matrix, $\boldsymbol{P}_{k+1|k}$ and $\boldsymbol{H}_{k+1|k}$ are given by:

$$\boldsymbol{P}_{k+1|k} = \boldsymbol{\Phi}_{k+1,k} \boldsymbol{P}_{k|k} \boldsymbol{\Phi}_{k+1,k}^{\mathrm{T}} + \boldsymbol{Q}_{k+1} \tag{11}$$

$$\boldsymbol{H}_{k+1|k} = [\partial \boldsymbol{h}(\boldsymbol{Z}_{k+1}, \boldsymbol{f}_{k+1}, k+1)/\partial \boldsymbol{Z}_{k+1}]_{\boldsymbol{Z}_{k+1} = \hat{\boldsymbol{Z}}_{k+1|k}} \tag{12}$$

where $\boldsymbol{\Phi}_{k+1,k}$ is the transition matrix of the extended state vector from $\boldsymbol{Z}_k$ to $\boldsymbol{Z}_{k+1}$, and $\boldsymbol{P}_{k|k}$ is given by:

$$\boldsymbol{P}_{k|k} = [\boldsymbol{I} - \boldsymbol{K}_k \boldsymbol{H}_{k|k-1}] \boldsymbol{P}_{k|k-1} [\boldsymbol{I} - \boldsymbol{K}_k \boldsymbol{H}_{k|k-1}]^{\mathrm{T}} + \boldsymbol{K}_k \boldsymbol{R}_k \boldsymbol{K}_k^{\mathrm{T}} \tag{13}$$

In the recursive solution above, $\boldsymbol{P}_{k|k}$ is the error covariance matrix of the estimated extended state vector, and the details of the EKF method are referred to Yang et al. [10]. To initiate the recursive solution, the initial values for the unknown extended state vector $\boldsymbol{Z}(t) = \{\boldsymbol{x}^{\mathrm{T}}, \dot{\boldsymbol{x}}^{\mathrm{T}}, \boldsymbol{\theta}^{\mathrm{T}}\}^{\mathrm{T}}$, including unknown parameters and unknown state vector, should be estimated. Likewise, the initial error covariance matrix $\boldsymbol{P}_{0|0}$ of the estimated extended state vector, the covariance matrix $\boldsymbol{R}$ of the measurement noise vector $\boldsymbol{v}(t)$, and the covariance matrix $\boldsymbol{Q}$ of the system noise vector $\boldsymbol{w}(t)$ should be assigned as will be described later.

Experimental Studies

Experimental tests

Rubber-bearings GZN110 supplied by Hengshui Zhentai Seismic Isolation Instrument CO., LTD were used as the base isolator of a structural model, and a mass with m = 132 kg is supported by rubber bearings as shown in Fig. 1(a). Two earthquake excitations will be used, including the El Centro and Kobe earthquakes. In the tests, the base-isolated structural model was placed on the shake table that simulated different kinds of earthquakes as shown in Figs. 1(a) and (b). During the tests, the shake table and the mass were each installed with one acceleration sensor and one displacement sensor to measure the responses. The absolute acceleration response of the mass a_1 and the earthquake ground acceleration a_d were measured.

Also, the displacements of the mass and the base were measured for the correlation study. The sampling frequency of all measurements is 200 Hz.

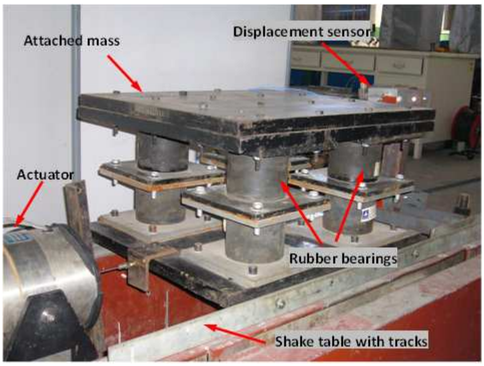

Fig. 1(a). Experimental setup (Global)

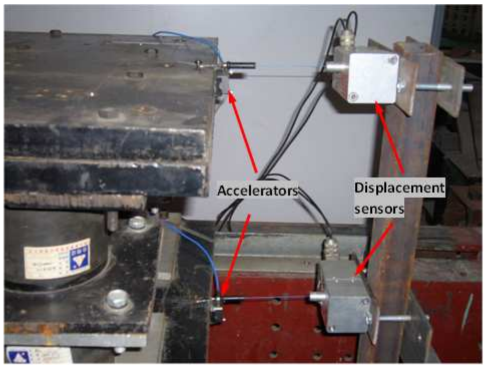

Fig. 1(b). Experimental setup (Local)

Experimental results

To identify the parameters of rubber-bearings, different unknown parameters in the Bouc-Wen model will be considered.

Bouc-Wen Model I (3 Unknown Parameters)

First, we consider the loop parameters, β γ and n to be constants, i.e., $\beta = 0.5$, $\gamma = 0.5$ and $n = 2$. Hence, the unknown parameters are c, k and α in which c and k are the linear damping and stiffness parameters and α is the ratio of post-yielding stiffness to pre-yielding stiffness. Then, the hysteretic nonlinear equation can be rewritten as:

$$\dot{z} = \dot{x} - 0.5|z|z - 0.5\dot{x}|z|^2 \tag{14}$$

The extended state vector in the EKF method is $\boldsymbol{Z}(t) = \{x, \dot{x}, z, c, k, \alpha\}^{\mathrm{T}}$, where x and $\dot{x}$ are the relative displacement and relative velocity, respectively, of the mass with respect to the shake table. The initial values used for $\boldsymbol{Z}$, $\boldsymbol{P}$, $\boldsymbol{Q}$ and $\boldsymbol{R}$ are: $\boldsymbol{Z}_{0|0} = \{0, 0, 0, 0.1, 20, 0.5\}^{\mathrm{T}}$, $\boldsymbol{P}_{0|0} = \mathrm{diag}\{[1,1,1,10^5,10^5,10^5]\}$, $\boldsymbol{R} = 1$, and $\boldsymbol{Q} = 10^{-7}\boldsymbol{I}_6$.

Case 1: El Centro earthquake

In this test, a scaled El Centro earthquake with a PGA of 0.4g is applied to the base. The measured earthquake ground acceleration a_d and the absolute acceleration response of the mass a_1 are shown in Fig. 2. Based on the acceleration measurements and the EKF solution, the identified unknown parameters are presented in Fig. 3. It is observed from Fig. 3 that the unknown parameters converge nicely after 3.5 seconds. Further, the identified displacements, including the absolute displacement and relative displacement (inter-story drift) of the mass, are shown in Fig. 4 as blue solid curves, whereas the measured displacements are shown as red dashed curves for comparison. It is observed from Fig. 4 that the identified displacements match the experimental ones well. Thus the parameters predicted in Fig. 3 can describe the nonlinear hysteretic characteristics well.

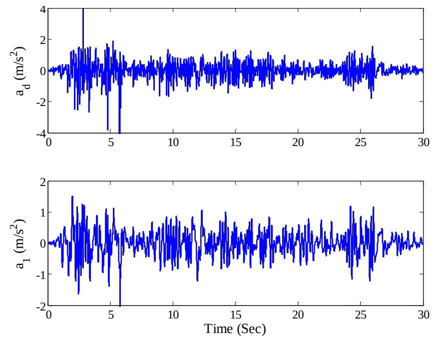

Fig. 2. Measured acceleration responses and shake table acceleration due to El Centro earthquake

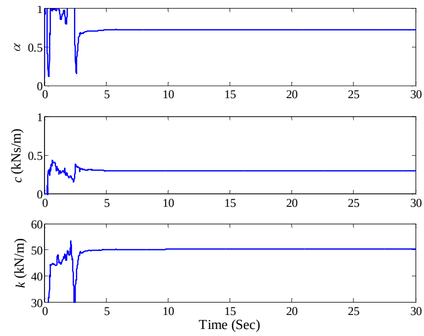

Fig. 3. The identified model parameters, case 1: El Centro earthquake

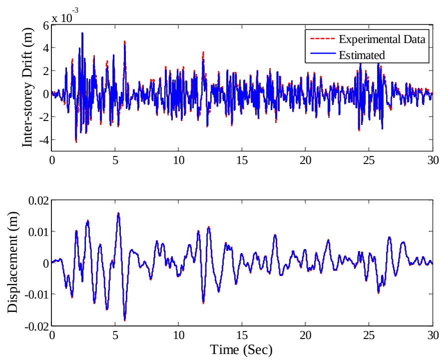

Fig. 4. The identified relative and absolute displacement, case 1: El Centro earthquake

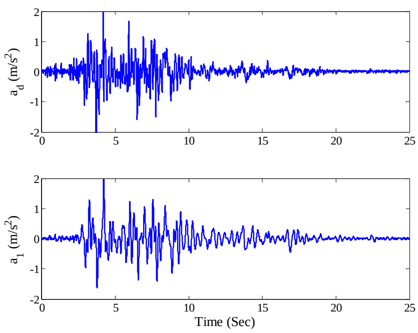

Fig. 5. Measured acceleration responses and shake table acceleration due to El Centro earthquake

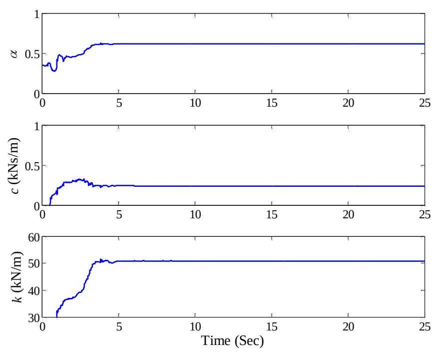

Fig. 6. The identified model parameters, case 2: Kobe earthquake

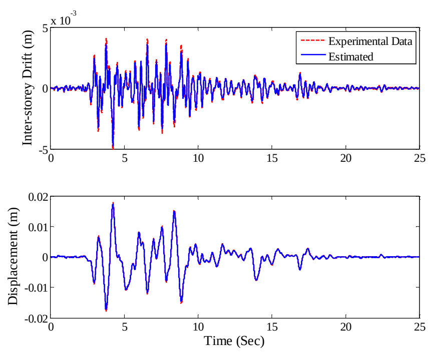

Fig. 7. The identified relative and absolute displacement, case 2: Kobe earthquake

Case 2: Kobe earthquake

In this test, a scaled Kobe earthquake with a PGA of 0.2g is applied to the base. The measured earthquake excitation a_d and the absolute acceleration response of the mass a_1 are shown in Fig. 5. Based on the acceleration measurements and the EKF solution, the identified parameters are presented in Fig. 6. A comparison between Figs. 3 and 6 indicates that the identified model parameters are identical under different excitations.

Bouc-Wen Model II (5 Unknown Parameters)

In this situation, we consider the parameter n to be 2.0, i.e., $n = 2$, and the other loop parameters, α, β and γ, to be unknown in Eqs. (2) and (3). Then, the extended state vector in the EKF method is $\boldsymbol{Z}(t)=\{x,\dot{x},z,c,k,\alpha,\beta,\gamma\}^{\mathrm{T}}$, where c, k, α, β and γ are the unknown parameters to be identified. The initial values used for $\boldsymbol{Z}$, $\boldsymbol{P}$, $\boldsymbol{Q}$ and $\boldsymbol{R}$ are: $\boldsymbol{Z}_{0|0}=\{0,0,0,0.1,20,0.5,0.5,0.5\}^{\mathrm{T}}$, $\boldsymbol{P}_{0|0}=\mathrm{diag}\{[1,1,1,10^5,10^5,10^5,10^5,10^5]\}$, $\boldsymbol{R} = 3$ and $\boldsymbol{Q}=10^{-7}\boldsymbol{I}_8$.

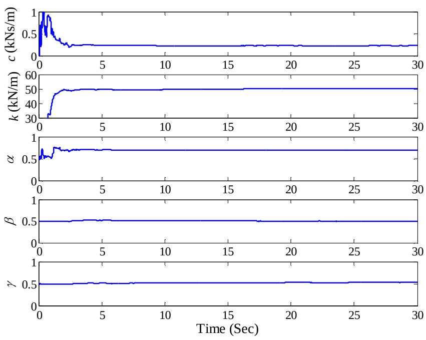

Fig. 8. The identified model parameters, case 3: El Centro earthquake

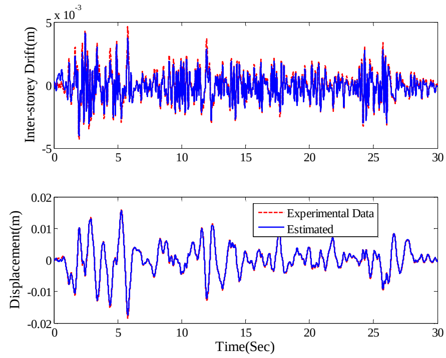

Fig. 9. The identified relative and absolute displacement, case 3: El Centro earthquake

Case 3: El Centro earthquake

Similar to case 1, a scaled El Centro earthquake with a PGA of 0.4g is applied to the base. Based on the acceleration measurements shown in Fig. 2 and the EKF solution, the identified parameters are presented in Fig. 10. Further, the identified displacements are shown in Fig. 11 as blue solid curves, whereas the measured displacements are represented as red dashed curves for comparison. It is observed from Fig. 11 that the identified displacements match the experimental ones well.

Case 4: Kobe earthquake

Similar to case 2, a scaled Kobe earthquake with a PGA of 0.2g is applied to the base. Based on the acceleration measurements shown in Fig. 5 and the EKF solution, the identified parameters are presented in Fig. 10. As observed from Fig. 10, all parameters converge nicely after 3.5 seconds. The identified displacements are provided in Fig. 11 as blue solid curves, whereas the measured displacements are shown as red dashed curves for comparison.

Bouc-Wen Model III (6 Unknown Parameters)

Experimental data obtained previously will be analyzed again by including the loop parameter n as an unknown parameter. In this case, the model involves 4 unknown loop parameters and 2 unknown linear parameters. Hence, the extended state vector in the EKF becomes $\boldsymbol{Z}(t)=\{x,\dot{x},z,c,k,\alpha,\beta,\gamma,n\}^{\mathrm{T}}$. The initial values for $\boldsymbol{Z}$, $\boldsymbol{P}$, $\boldsymbol{Q}$ and $\boldsymbol{R}$ are: $\boldsymbol{Z}_{0|0}=\{0,0,10^{-12},0.1,40,0.5,0.5,0.5,2\}^{\mathrm{T}}$, $\boldsymbol{P}_{0|0}=\mathrm{diag}\{[1,1,1,10^3,10^3,10^3,10^3,10^3,10^3]\}$, $\boldsymbol{R}$ = 10 and $\boldsymbol{Q}=10^{-7}\boldsymbol{I}_9$.

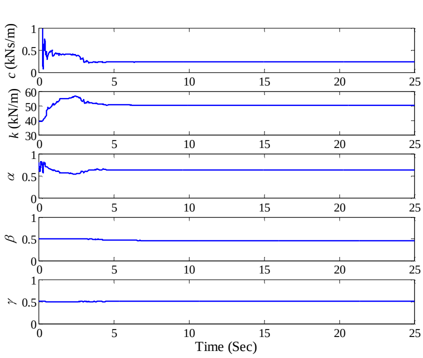

Fig. 10. The identified model parameters, case 4: Kobe earthquake

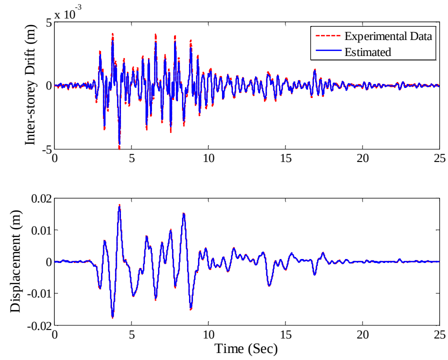

Fig. 11. The identified relative and absolute displacement, case 4: Kobe earthquake

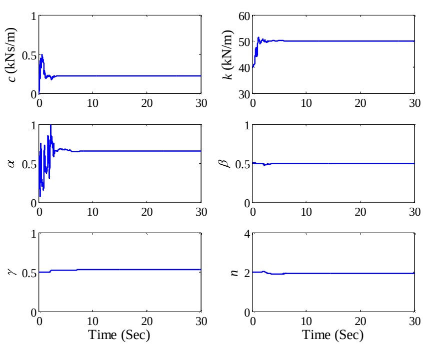

Fig. 12. The identified model parameters, case 5: El Centro earthquake

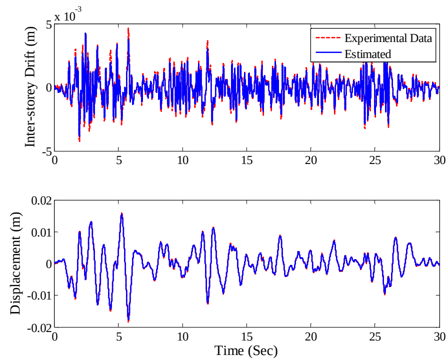

Fig. 13. The identified relative and absolute displacement, case 5: El Centro earthquake

Case 5: El Centro earthquake

Based on the measured data in Case 1 for the El Centro earthquake excitation and the EKF approach, the identified results are shown in Figs. 12 and 13, respectively, for the unknown parameters and the displacement responses. A comparison of Figs. 3, 8 and 12 indicates that the identified parameters are identical for all Bouc-Wen Model I and Bouc-Wen Model II as well as Bouc-Wen Model III for the El Centro earthquake excitation.

Case 6: Kobe earthquake

Based on the measured data in Case 2 for the Kobe earthquake excitation and the EKF approach, the identified results are shown in Figs. 14 and 15 respectively, for the unknown parameters and the displacement responses. A comparison of Figs. 6, 10 and 14 indicates that the identified parameters are identical for both Bouc-Wen Model I and Bouc-Wen Model II as

© VIBROENGINEERING. JOURNAL OF VIBROENGINEERING. MARCH 2012. VOLUME 14, ISSUE 1. ISSN 1392-8716

well as Bouc-Wen Model III for the Kobe earthquake excitation. Finally, an examination of Figs. 3, 8, 12, 6, 10 and 14 reveals that all the identified parameters are about the same for all Bouc-Wen Models and for all earthquake excitations. Likewise, the predicted displacement responses correlate very well with the experimental data as presented in Figs. 4, 7, 9, 11, 13 and 15.

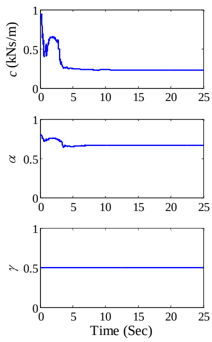

Fig. 14. The identified model parameters, case 6: Kobe earthquake

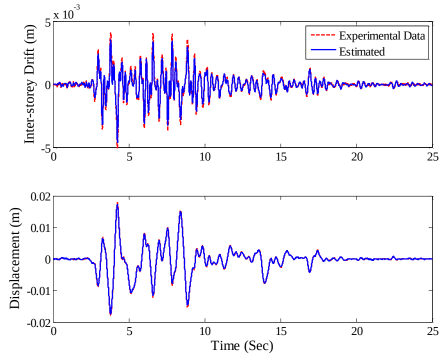

Fig. 15. The identified relative and absolute displacement, case 6: Kobe earthquake

Conclusions

In this paper, experimental studies have been conducted for the system identification of nonlinear hysteretic rubber-bearings. Experimental tests of a rubber-bearing isolator under El Centro and Kobe earthquakes have been performed to generate the acceleration response data for the system identification purpose. The Bouc-Wen models with 3, 5 and 6 unknown parameters, respectively, have been investigated to represent the hysteretic behavior of rubber-bearing isolators. The EKF approach has been used to identify the nonlinear parameters of the Bouc-Wen models for the rubber-bearing isolators, including the equivalent stiffness, damping coefficient and hysteretic parameters. Our experimental studies demonstrate that the Bouc-Wen models are capable of describing the nonlinear behavior of rubber-bearing isolators, and that the EKF approach is quite effective in identifying nonlinear hysteretic parameters.

Acknowledgements

This research is partially supported by the National Natural Science Foundation of China under Grant No. 10572058, the Funds for International Cooperation and Exchange of the National Natural Science Foundation of China under Grant No. 61161120323, and US National Science Foundation Grant No. CMMI-0853395. And the writers would like to thank the support from Hengshui Zhentai Seismic Isolation Instrument Co., Ltd.

References

[1] **Kelly J. M.** Earthquake-Resistant Design with Rubber. Second Edition, London, 1997.

[2] **Komodromos P.** Seismic Isolation for Earthquake-Resistant Structures. WIT Press, Ashurst Lodge, Inc., 2000.

[3] **Jangid R. S., Datta T. K.** Seismic behavior of base isolated building – a state-of-the-art-review. Structures and Buildings, Vol. 110, 1995, p. 186-203.

[4] **Buckle I. G., Nagarajaiah S., Ferrell K.** Stability of elastomeric isolation bearings: Experimental study. Journal of Structural Engineering, ASCE, Vol. 128, Issue 1, 2002, p. 3-11.

[5] **Furukawa T., Ito M., Noori M. N.** System identification of base-isolated building using seismic response data. Journal of Engineering Mechanics, ASCE, Vol. 131, Issue 3, 2005, p. 268-273.
[6] **Lin J. W., Betti R., Smyth W. A., Longman R. W.** On-line identification of nonlinear hysteretic structural system using a variable trace approach. Earthquake Engineering and Structural Dynamics, Vol. 30, 2001, p. 1279-1303.
[7] **Yang J. N., Lin S.** Identification of parametric variations of structures based on least square estimation and adaptive tracking technique. Journal of Engineering Mechanics, ASCE, Vol. 131, Issue 3, 2005, p. 290-298.
[8] **Yang J. N., Pan S., Lin S.** Least square estimation with unknown excitations for damage identification of structures. Journal of Engineering Mechanics, ASCE, Vol. 133, Issue 1, 2007, p. 12-21.
[9] **Sato T., Honda R., Sakanoue T.** Application of adaptive Kalman filter to identify a five story frame structure Using NCREE experimental data. Proceedings of Structural Safety and Reliability, ICOSSA2001, 2001, Swets & Zeitinger: Lisse, CD-ROM, 7 pages.
[10] **Yang J. N., Lin S. L., Huang H. W., Zhou L.** An adaptive extended Kalman filter for structural damage identification. Journal of Structural Control and Health Monitoring, Vol. 13, 2006, p. 849-867.
[11] **Zhou L., Wu S. Y., Yang J. N.** Experimental study of an adaptive extended Kalman filter for structural damage identification. Journal of Infrastructure Systems, ASCE, 14(1), 2008, 42-51.
[12] **Wu M. L., Smyth A.** Real-time parameter estimation for degrading and pinching hysteretic models. International Journal of Non-Linear Mechanics, Vol. 43, Issue 4, 2010, p. 822-833.
[13] **Yin Q., Zhou L.** Non-linear structural identification using a recursive model reference adaptive algorithm. Journal of Vibration Engineering, Vol. 19, Issue 3, 2006, p. 341-345.
[14] **Yang J. N., Huang H., Lin S.** Sequential non-linear least-square estimation for damage identification of structures. International Journal of Non-Linear Mechanics, Vol. 41, 2006, p. 124-140.
[15] **Yin Q., Zhou, L., Wang X. M.** Parameter identification of hysteretic model of rubber-bearing based on sequential nonlinear least-square estimation. Earthquake Engineering and Engineering Vibration, Vol. 9, Issue 3, 2010, p. 375-383.
[16] **Yang J. N., Huang H. W., Pan S. W.** Adaptive quadratic sum-squares error for structural damage identification. Journal of Engineering Mechanics, ASCE, Vol. 135, Issue 2, 2009, p. 67-77.
[17] **Huang H., Yang J. N., Zhou L.** Adaptive quadratic sum-squares error with unknown inputs for damage identification of structures. Journal of Structural Control and Health Monitoring, Vol. 17, Issue 4, 2010, p. 404-426.
[18] **Sato T., Chung M.** Structural identification using adaptive Monte Carlo filter. Journal of Structural Engineering, JSCE, Vol. 51(A), 2005, p. 471-477.
[19] **Chang C. C., Shi Y. F.** Identification of time-varying hysteretic structures using wavelet multiresolution analysis. International Journal of Non-Linear Mechanics, Vol. 45, Issue 1, 2010, p. 21-34.
[20] **Ma F., Zhang H., Bockstedte A., Foloente G. C., Paevere P.** Parameter analysis of the differential model of hysteresis. Journal of Applied Mechanics, ASCE, Vol. 71, 2004, p. 342-349.
[21] **Chen B. J., Tsai C. S., Chung L. L., Chiang T. C.** Seismic behavior of structures isolation with a hybrid system of rubber bearings. Structural Engineering and Mechanics, Vol. 22, Issue 6, 2006, p. 761-783.